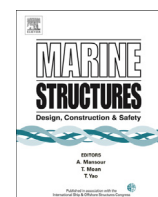




Contents lists available at ScienceDirect

Marine Structures

journal homepage: www.elsevier.com/locate/marstruc

Validation of naval vessel spectral fatigue analysis using full-scale measurements

Ian Thompson

Defence Research and Development Canada, Atlantic Research Centre, 9 Grove Street, Dartmouth, Nova Scotia, B2Y 3Z7, Canada

ARTICLE INFO

Article history:

Received 30 November 2015

Received in revised form 11 April 2016

Accepted 24 May 2016

Available online xxx

Keywords:

Fatigue

Naval vessel

Full-scale measurement

Spectral approach

Spectral fatigue analysis

Wave spectrum

ABSTRACT

Full-scale measurements taken during a naval vessel sea trial are compared to calculated stress spectra and associated fatigue damage estimates using linear frequency-domain hydrodynamic and finite element analysis codes. Results were generated using four different wave spectrum models to better understand their influence on fatigue damage estimates. The results using measured two-dimensional wave spectra were most similar to measurements, but the agreement with measurements for each of the spectrum models was acceptable. Significant improvement in calculation accuracy was observed when adding a spreading function to longcrested wave spectra. The use of $\pm 90^\circ$ as the extent of wave spreading gave results with minimal differences from the use of measured spreading angles. The agreement between measurements and calculations using longcrested wave spectra with a constant spreading function is fortunate because available seaway data are commonly limited to wave height and period combinations. The results of this study suggest the spectral fatigue analysis method can be used to generate reasonable estimates of stress spectra and resulting fatigue damage for a naval vessel.

Crown Copyright © 2016 Published by Elsevier Ltd. This is an open access article under the CC BY-NC-ND license (<http://creativecommons.org/licenses/by-nc-nd/4.0/>).

1. Introduction

Ship hulls are exposed to millions of cycles of varying wave forces over their lives. The load cycles on a ship's hull lead to the formation of fatigue cracks; this can be exacerbated in naval vessels which often have lighter scantlings due to the use of high-strength steels. The management of cracks in warships, which are typically of lightweight construction and frequently operate in severe wave conditions, is a considerable maintenance issue [1]. Repairs to prevent these cracks from growing into sites of potential catastrophic failure can be very costly and reduce the availability of the ship. A tool based on spectral fatigue analysis could be used to predict the onset of fatigue cracks and to identify the critical areas of a hull structure in order to prevent fatigue problems through better design. The same tool could be applied to in-service ships to determine the remaining fatigue life based on operational history, to inform inspection plans, and to assess the impact of engineering changes and damage, e.g., corrosion, on the fatigue life of the vessel.

Spectral fatigue analysis involves determining the hydrodynamic forces on the ship hull in the frequency domain due to waves in operating conditions, then calculating the resulting stress transfer functions. The stress spectra and their frequency of occurrence can be determined by combining the stress transfer functions with the amount of time in each of the considered sea states, ship speeds, and headings relative to the waves. The fatigue initiation life can be estimated by combining the stress spectra and S-N curves assuming linear cumulative damage and a narrow-banded response. Linear hydrodynamic loads and

E-mail address: ian.thompson@drdc-rddc.gc.ca.

<http://dx.doi.org/10.1016/j.marstruc.2016.05.006>

0951-8339/Crown Copyright © 2016 Published by Elsevier Ltd. This is an open access article under the CC BY-NC-ND license (<http://creativecommons.org/licenses/by-nc-nd/4.0/>).

Please cite this article in press as: Thompson I, Validation of naval vessel spectral fatigue analysis using full-scale measurements, Marine Structures (2016), <http://dx.doi.org/10.1016/j.marstruc.2016.05.006>

responses are assumed in this study but non-linearities (e.g. mean stress effects) can be considered with the use of correction factors. Ref. [2] provides an overview of spectral fatigue analysis for ships.

Ship classification societies have developed guidelines to perform spectral fatigue analysis [3–5] and analyses of commercial ship components are well documented in the open literature. Examples include analyses of a longitudinal pad coaming using requirements from different class societies [6] and a comparative study of a hatch cover bearing pad [7]. Damage estimates using Pierson-Moskowitz and JONSWAP wave spectrum models were presented in a parametric study of a liquefied natural gas carrier showing up to 20% difference between the models for two sea states [8]. An analysis of a dredging barge structural detail was conducted using linear strip theory and hull girder analysis and the results were found to differ significantly with calculations based on International Association of Class Societies recommendations [9]. Damage estimates from tests of an instrumented flexible containership model were compared with calculated damage estimates [10]. The numerical methods yielded estimates with good agreement of wave-frequency damage but overpredictions of wave-induced vibrations and the associated damage. Full-scale measurements during three sea states at two locations on a container ship were used to compare estimates of damage based on several different modeling techniques with estimates based on measurements [11]. Damage estimates varied from 15% lower than those based on measurements to 115% over. The influence of wave spreading was also compared for an assumed seaway and found to be substantial for beam seas.

The availability of literature that compares calculated values of stress spectra or damage estimates with full-scale measurements is limited for commercial vessels but fewer examples are available for naval vessels. The lone exception known to the author involved the United States Coast Guard maritime cutters analyzed in the VALID Joint Industry Project. The model-scale and full-scale work are described in Ref. [12]. Although the cutters are not naval vessels, they have a hull form similar to a frigate. In a comparison of the loading, the measured vertical bending moments were compared to vertical bending moments calculated using several different hydrodynamic codes [13]. The hydrodynamic codes typically overpredicted vertical bending moments, but were within 25% for significant wave heights up to 2.5 m. Stresses and damage were calculated but not explicitly compared.

The motivation for this work was to validate the use of the combination of a linear frequency-domain hydrodynamics code with a linear FE solver to calculate estimates of fatigue damage for a naval vessel. Spectral fatigue analysis includes a large number of simplified aspects, some of which introduce more error than others. These include, but are not limited to: representation of the seaway, representation of the main characteristics of the ship in hydrodynamic and FE models, the use of linear hydrodynamic and FE codes, the operational profile of the ship, S-N curves, stress concentration factors, and the probability of fatigue failure [4,14]. Although they were not considered in this study, vibration stresses from springing and whipping can contribute to fatigue damage as well. The second motivation for this study was to improve the understanding of the influence of the fidelity of the seaway representation. Precise wave measurements were taken for this sea trial, but typically wave statistics with far fewer details are used for spectral fatigue analyses.

In this paper, stress spectrum parameters and damage estimates derived from strain measurements taken during a naval vessel sea trial are compared with values calculated using spectral fatigue analysis software. The comparisons are used to assess the accuracy of the technique with the available tools and to better understand the impact of making simplifications of the seaway representation. The considered ship is a longitudinally-stiffened displacement hull built to Canadian Naval Standards which lead to similar structural designs as those generated using classification society naval rules. Root mean square (RMS) stress, zero-upcrossing frequency, and damage estimates are compared using measured values and calculated values. The two stress spectra parameters were the primary comparisons for validation since they can be derived directly from the strain measurements while fatigue damage estimates involve more manipulations and assumptions. Although the fatigue damage is typically the value of most interest to analysts, errors in either the RMS stress or zero-upcrossing frequency contribute to the error in its calculation. Comparing the fatigue damage estimates shows the agreement in this parameter of most interest based on the observed level of error in the stress spectra. Four types of wave spectrum models are used for comparison of results: long-crested without directional spreading; long-crested with cosine squared spreading and a spreading angle of 90°; long-crested with cosine squared spreading and spreading angles measured for each trial run; and the full directional wave spectra measured by a wave buoy.

This paper is an extension of preliminary work presented in Ref. [15] where the measured stress spectra were compared with calculated values using a long-crested wave spectrum model and measured directional wave spectra. In the current work, the validation is extended to include the primary goal of a spectral fatigue analysis: the predicted fatigue damage. The extension of work also includes changes to the hydrodynamic calculations by improving the roll damping and assessing additional wave spectrum models. The roll damping in the present study was specified based on a seakeeping analysis of ship motions. One of the gauge locations considered in Ref. [15] was omitted (s36) as the structural details in the FE model are incorrect and accurate details are not available.

2. Methodology

Values derived from strain measurements taken on a naval vessel sea trial are compared with those calculated using software that combines hydrodynamic and finite element calculations within a spectral fatigue analysis framework. The experimental strain values used in this study were taken during a sea trial that began on the Grand Banks off Newfoundland, Canada, moved south of the Avalon Peninsula, and completed east of Sable Island. Seventy-five trial runs with durations between 20 and 30 min were conducted where the speed (nominally 10 or 20 knots) and heading were held constant. The

significant wave heights varied between 0.7 m and 6.1 m and a variety of headings into the waves were experienced. A freely floating Triaxys wave buoy was used to measure the waves and fourteen uniaxial strain gauges were applied longitudinally at three cross sections approximately 20, 50, and 65% of the length between perpendiculars (L_{pp}) measured from the forward perpendicular. The strain gauges were sampled at 50 Hz then signals above 20 Hz were filtered out to prevent aliasing. Whipping contributions were filtered out and the RMS strain and zero-upcrossing frequency values were calculated for each trial run. Strain values were converted to stress using Hooke's Law because uniaxial gauges were used.

A sketch of the approximate gauge locations is shown in Fig. 1 and Table 1 shows the details of the strain gauge locations. Gauges were located on longitudinal members on the web of the local structure near the adjacent shell or deck plating. The areas selected are at the extreme fibers of the hull girder away from sources of stress concentration. The strain gauges were not near stress concentrations so the stresses were not high; as such, these areas are not prone to fatigue damage. All of the available data from the 75 trial runs were used for each gauge but problems during the sea trial prevented taking measurements from five strain gauges during some trial runs. Gauge s17 took measurements on 23 trial runs, gauge s19 functioned on 57 runs, gauge s15 on 69 runs, gauge s30 on 72 runs, and gauge s18 on 74 runs.

Calculated values of RMS stress, zero-upcrossing frequency, and damage estimates were generated using software developed within Cooperative Research Ships (CRS). A whole-ship hydrodynamic model was created that contained 11028 nodes and 10134 panels. The June 2014 version of PRECAL_R [16], the linear three-dimensional frequency domain hydrodynamic code developed within CRS, was used with this model to calculate the nodal forces under each combination of considered speeds, headings relative to the waves, and wave frequencies. The two nominal trial speeds (10 knots and 20 knots), 24 headings (15° increments), and 38 wave frequencies (0.1 rad/s increments from 0.1 to 0.4 rad/s and 1.6–2.6 rad/s and 0.05 rad/s increments between 0.4 rad/s and 1.6 rad/s) were used to create 1824 unique load cases, or combinations of parameter values.

STRUC_R version 2.4.43 [17], the CRS spectral fatigue analysis code, was used to couple the hydrodynamic model and FE model, interact with the FE solver, and calculate stress spectra. Nodal forces from the 1824 load cases generated with PRECAL_R were applied to a global FE model of the entire ship structure and the displacements and stresses calculated using the VAST FE solver [18]. Topdown, or global-local, analysis was used to determine the stresses for each load case in detailed local FE models of each strain measurement location. The boundary conditions of the local models were obtained from the global model solution. This involved applying the displacements at nodal locations on the global FE model to coincident local master nodes in the local models that had a common boundary with the global model. Other local nodes sharing a common boundary with the global model were considered slave nodes; their displacements were calculated using linear interpolation between the master nodes. The mesh size of the global FE model, shown in Fig. 2, was equivalent to approximately one quarter of the frame spacing, yielding a total of 71854 nodes and 156636 elements (primarily shell and beam elements). Local refined models were created for each strain gauge location and typically extended to the next frames longitudinally and to adjacent stiffeners transversely. Typically in the local models, there were thirty elements along the length of each coincident global element, resulting in local models with between 4000 nodes and elements to 28000 nodes and 29000 elements. This level of refinement produced local elements in the area of interest similar in size to the strain gauges used. The local model for gauge s26 is shown as an example in Fig. 3.

The wave measurements were modeled in four different ways: a uni-directional spectrum without spreading (1-d), a uni-directional spectrum with a spreading function and constant spreading angle (1-d with 90° spreading angle), a uni-directional spectrum with the same spreading function and the measured spreading angle (1-d with measured spreading angle), and the measured two-dimensional wave spectra (2-d). The simplest model used the measured significant wave

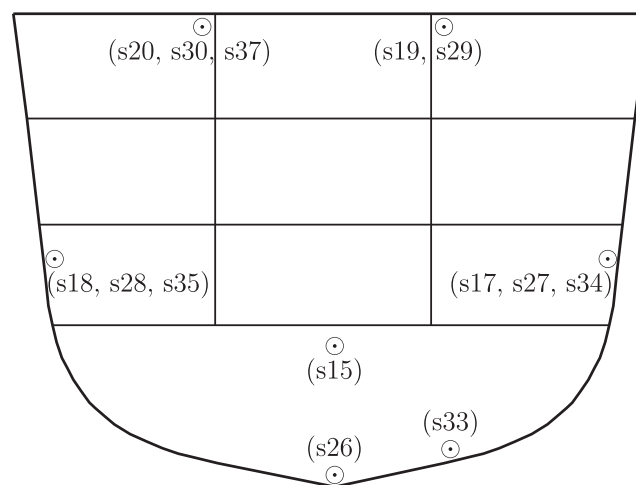
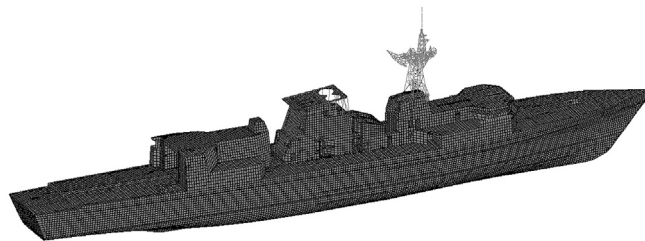
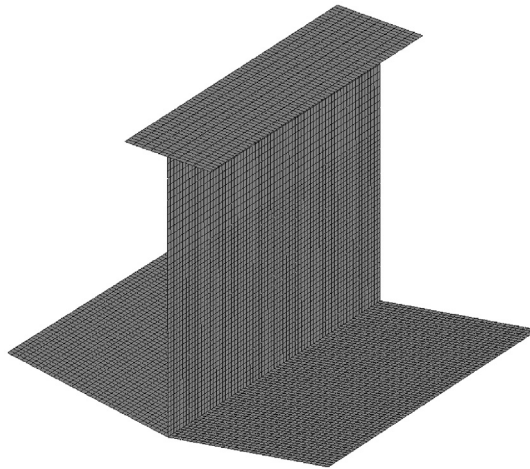


Fig. 1. Approximate locations of strain gauges.

Table 1

Strain gauge locations.

Gauge number	Longitudinal position (% of L_{pp} from bow)	Gauge location details
s15	20	Top of centerline longitudinal bulkhead under #4 deck
s17	20	Side shell longitudinal 20 - port
s18	20	Side shell longitudinal 20 - starboard
s19	20	Main deck girder - port
s20	20	Main deck girder - starboard
s26	50	Bottom of keel girder
s27	50	Side shell longitudinal 20 - port
s28	50	Side shell longitudinal 20 - starboard
s29	50	Longitudinal bulkhead mid-way between centerline and side shell - port
s30	50	Longitudinal bulkhead between centerline and side shell starboard
s33	65	Side shell longitudinal 8 - port
s34	65	Side shell longitudinal 20 - port
s35	65	Longitudinal 20 - starboard
s37	65	Longitudinal bulkhead - between centerline and side shell - starboard

**Fig. 2.** Global FE model.**Fig. 3.** Local FE model of gauge s26.

height and peak period in the two-parameter Pierson-Moskowitz spectrum [19]. This uni-directional approximation is referred to as 1-d and may be used for calculations based on wave statistics when no spreading of the waves is assumed. A cosine-squared spreading function was used with the same two-parameter Pierson-Moskowitz spectra for two wave spectrum models. The spreading function is shown in Eq. (1) where θ is the heading angle relative to the principal wave direction and γ_s is the spreading angle in radians.

$$G(\theta) = \frac{1}{\gamma_s} \cos^2 \left(\frac{\theta}{\gamma_s} \frac{\pi}{2} \right) \quad \text{for } |\theta| \leq \gamma_s \quad (1)$$

When $|\theta| > \gamma_s$, $G(\theta) = 0$.

The area under the spreading function is unity, as required to avoid modification of the total energy in the seaway representation.

In one of the models using the spreading function, the spreading angle was assumed to be 90° , as recommended by DNV-GL [20]. This is referred to as 1-d with 90° spreading angle and would be used when no information is available about the wave spreading. The spreading angle for each of the trial runs was determined based on buoy measurements and found to vary between 52° and 163° , with an average of 98° and a standard deviation of 32° . These values were used in the cosine-squared spreading function along with the two-parameter Pierson-Moskowitz spectrum as the third wave model, referred to afterwards as 1-d with measured spreading. The final method is the measured two-dimensional wave spectra. This is the most accurate representation of the sea state, but requires far more information than the other methods and is only available if the wave conditions are measured. The 2-d spectrum requires spectral energy density values at each combination of heading and wave frequency; in this case, 123 frequencies up to 3.8 rad/s and 120 heading angles. By comparison, the wave spreading methods discussed earlier require only two wave spectrum parameters and the spreading angle and exponent.

The wave buoy provided the measured two-dimensional wave spectrum, as mentioned above, as well as the peak period and significant wave height for each trial run. The peak period was the wave period with the highest energy and the significant wave height was determined from the 2-d measurements as $4\sqrt{M_0}$ where M_0 is the zeroth spectral moment. The spectral moments were calculated using Eq. (2), where ω is the angular frequency, $S(\omega)$ is the wave spectrum, and n is the order of the spectral moment.

$$M_n = \int_0^\infty \omega^n S(\omega) d\omega \quad (2)$$

Eq. (2) applies to long-crested waves; for short-crested waves the integration must be performed with respect to the spreading angle as well since the wave spectrum is a function of both frequency and spreading angle.

To ensure each type of seaway model contributed similar amounts of energy at similar frequencies for each trial run, the zeroth and second spectral moments of the wave spectra were compared. The second spectral moment was calculated because the zero-upcrossing frequency can be estimated as $2\pi\sqrt{M_2/M_0}$.

Stress transfer functions for each strain gauge location were generated for all combinations of speed and heading relative to the waves using topdown analysis, as described above. The stress spectrum for each strain gauge was calculated for each trial leg by multiplying the square of the appropriate stress transfer functions and the wave spectrum for the trial leg. The RMS stress and zero-upcrossing frequency can be estimated from the stress spectral moments as $\sqrt{M_0}$ and $\sqrt{M_2/M_0}$, respectively.

To make the most direct comparison, thus minimizing assumptions and manipulations, the measured longitudinal strain should have been compared with the calculated longitudinal strain. However, at present, STRUC_R is limited to generating transfer functions for different components of stress, rather than strain, which makes this comparison difficult. In this study, the longitudinal stress calculated with STRUC_R is compared to the stress calculated using Hooke's Law from the measurements of longitudinally-mounted uniaxial strain gauges. This is reasonable provided that the transverse strain is very small relative to the longitudinal strain.

Damage estimates for both measured and calculated stress spectra were calculated for each trial leg using Eq. (3) [5], where D is the damage estimate, T is the duration, ω_z is the zero-upcrossing frequency, Γ is the gamma function, and m and K are the parameters for a linear S-N curve.

$$D = \frac{T\omega_z}{K} \left(2\sqrt{2M_0}\right)^m \Gamma(1 + m/2) \quad (3)$$

For this study, a linear S-N curve was selected with m set to 3 and $\log_{10} K$ set to 12.436, as suggested for base material in a corrosive environment in Ref. [4]. This assumes the coating was not intact.

The calculated values of RMS stress, ω_z , and damage were compared with the values derived from strain gauge measurements on the sea trial using a Matlab script. Several different methods were used to compare the measured and calculated values, since no single validation metric was found that could completely characterize the accuracy of the predictions. The first method involved linear regression through the origin to determine the slope of the best-fit line and the coefficient of determination (R^2). The measured values were the independent variables and calculated values were the dependent variables. As regression was through the origin, $R^2 = \sum(\text{fitted values})^2 / \sum(\text{STRUC_R values})^2$ [21]. Differences between calculated values and those derived from measurements have also been assessed using the coefficient of variation of root mean square deviation (CV(RMSD)), calculated as shown in Eq. (4) (where N is the number of trial runs).

$$\text{CV(RMSD)} = \frac{\sqrt{\frac{\sum_{i=1}^N (\text{Calculated} - \text{Measured})^2}{N}}}{\text{Mean of measured parameter}} \quad (4)$$

Lower values of CV(RMSD) indicate better agreement with measurements. The mean of the ratio of the STRUC_R values divided by trial values was calculated. These means complement the regression slopes which can be overly influenced by measurements at outlying independent variable points. Although the values of the means differed from the regression slopes, they did not lead to different conclusions. These values have been omitted for brevity.

The calculated damage estimates for each gauge were summed over all of the trial runs and divided by the total damage estimated for each gauge using measured parameters. This provides an estimate of the accuracy of the calculated damage over the entire trial as it reduces the influence of conditions that would not cause a significant amount of structural fatigue damage.

3. Results

The spectral moments of the four seaway models are compared below. The RMS stress, zero-upcrossing frequency, and damage estimates calculated with each of the seaway models are compared to values of each parameter based on measurements. The influence of using longitudinal stress in this study is also assessed.

3.1. Comparison of seaway spectral moments

The spectral moments (Eq. (2)) of the seaway models were compared to evaluate potential differences. The long-crested spectra (with and without spreading) had M_0 values that were, on average, 6% lower than the M_0 values of the 2-d spectra. The ratio of the 1-d to 2-d M_0 values had a standard deviation of 0.04. The average of the ratio of the M_2 values (1-d values/2-d values) was 1.02 and the standard deviation was 0.19. Generally, although the M_0 values were similar, indicating the energy in the spectra was similar, the peak value of the 2-d spectra was higher than those of the long-crested spectra. A typical example is shown in Fig. 4.

3.2. Stress spectra parameters and damage estimates for each seaway model

Comparisons of the calculated results using the 1-d (without spreading) and 2-d wave spectrum models to those based on the strain gauge measurements are shown in Tables 2–4. The results for each gauge and the average (avg), standard deviation (std dev), minimum value (min), and maximum value (max) of each parameter are presented. Table 2 compares the RMS stress results. The regression slopes indicate that calculated RMS stress is 3–5% less than the measured values on average, but there are underpredictions by as much as 34% and overpredictions up to 44%. Table 3 shows the zero-upcrossing frequency results. The regression slopes for the zero-upcrossing frequencies show that the calculated values are typically lower than measured: by 18% on average for the 1-d spectra and 4% on average for the 2-d spectra. The regression slopes did not vary between gauges as much as they did for the RMS stress. Table 4 shows the results of fatigue damage estimates created by combining RMS stress, zero-upcrossing frequency, and S-N curve parameters (Eq. (3)). The sums of the damage estimates over all trial runs show that the 1-d wave spectra calculations overpredict values based on measurements by 47% on average and result in significant outliers. The sums of the damage estimates for the 2-d wave spectra showed a 3% underprediction on average with less variation than the 1-d results.

Example plots of the 2-d results of strain gauges s15 and s26 are shown for the RMS stress (Figs. 5 and 6, respectively), zero-upcrossing frequency (Figs. 7 and 8, respectively), and damage estimates (Figs. 9 and 10, respectively) following the table with each respective value. Gauge s15 was at the cross section nearest the bow at the top of the centerline longitudinal bulkhead under #4 deck. Gauge s26 was at the bottom of the keel girder near midship. These two sets of plots show the calculated results with some of the poorest agreements with measurements (gauge 15) and some of the best agreements with measurements (gauge s26).

The results for individual gauges for the wave spectrum models which included spreading have been omitted for brevity, but descriptive statistics are provided in Table 5 for the wave model using 90° as the spreading angle and Table 6 for the wave model using the measured wave spreading angle. Both tables show average regression slopes for RMS stress, zero-upcrossing

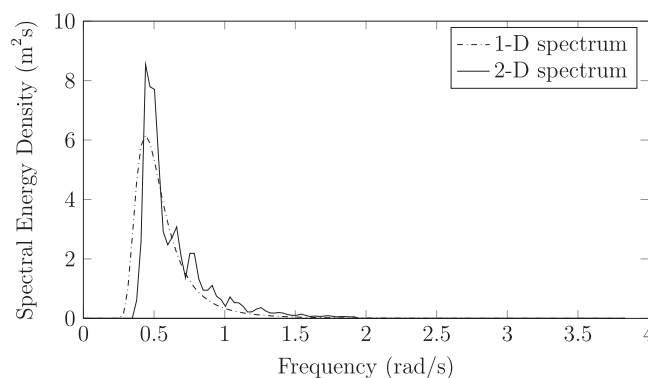


Fig. 4. Example wave spectrum showing 1-d and 2-d representations. Significant wave height was 5.5 m, peak frequency was 0.44 rad/s.

Table 2

Comparison of calculated and measured RMS stress (STRUC_R result/gauge measurement) for 1-d and 2-d wave spectra.

Strain Gauge	Regression slope		R^2		CV (RMSD)	
	1-d	2-d	1-d	2-d	1-d	2-d
15	1.44	1.35	0.91	0.98	0.73	0.47
17	0.94	0.81	0.92	0.94	0.30	0.29
18	0.70	0.78	0.84	0.96	0.47	0.30
19	0.66	0.69	0.91	0.98	0.48	0.40
20	0.77	0.71	0.95	0.97	0.34	0.38
26	1.05	0.98	0.91	0.99	0.39	0.13
27	0.96	1.05	0.81	0.97	0.51	0.19
28	0.94	1.04	0.80	0.98	0.51	0.18
29	0.98	0.92	0.91	0.99	0.37	0.16
30	1.05	0.99	0.91	0.99	0.39	0.12
33	1.22	1.14	0.91	0.99	0.52	0.22
34	0.80	0.86	0.84	0.98	0.44	0.21
35	0.83	0.87	0.88	0.98	0.39	0.21
37	1.23	1.16	0.91	0.99	0.54	0.23
avg	0.97	0.95	0.89	0.98	0.46	0.25
std dev	0.22	0.19	0.05	0.01	0.11	0.11
min	0.66	0.69	0.80	0.94	0.30	0.12
max	1.44	1.35	0.95	0.99	0.73	0.47

frequency, and damage estimates that are closer to unity than the corresponding values for the 1-d spectra without spreading. The results for the two wave spectra using different spreading functions yielded very similar results.

3.3. Use of longitudinal stress for comparison

The error introduced by using only longitudinal strains to derive the experimental stress was estimated by comparing the longitudinal and transverse stresses predicted by the software using 2-d wave spectra. The average RMS transverse stress for all gauges and all trial leg runs was 1.5% of the longitudinal stress. The RMS longitudinal strain was estimated by subtracting the product of the RMS transverse stress and Poisson's ratio (0.3) from the longitudinal stress and dividing the result by the elastic modulus. A regression analysis was conducted comparing the measured and calculated RMS longitudinal strain, similar to the stress comparisons. The statistics generated from the strain comparisons had trivial differences from the stress comparisons shown in Table 2 for the 2-d spectra.

4. Discussion

The comparison of the spectral moments of the 1-d and 2-d seaway models are discussed, as is the absence of transverse strain measurements in calculations of measured longitudinal stress. The agreement of the different measurement locations are discussed relative to one another for all the wave spectrum models. The 1-d and 2-d results are compared to one another, the results using two spreading functions are compared to one another, and the results generated using spreading functions are compared to the 1-d and 2-d results.

4.1. Comparison of seaway models

The similarity of the zeroth and second spectral moments for the 1-d and 2-d wave spectra suggests that the two methods of representing the seaway had similar amounts of energy at similar frequencies. There are differences due to the accuracy of the seaway representation, particularly with respect to spreading, but the 1-d model was a representative simplification of the 2-d measurements. Although the spectral shapes are somewhat different in some cases, this is one of the outcomes of using a simplified mathematical formula to represent a seaway.

4.2. Use of measured longitudinal strain to calculate longitudinal stress

The low magnitude of the calculated transverse stresses suggests the use of longitudinal stresses calculated only using longitudinal strains for comparison is reasonable. The similarity of the statistics generated for the estimated longitudinal strain with those of the calculated longitudinal stress suggests this simplification does not introduce a significant amount of error.

Table 3

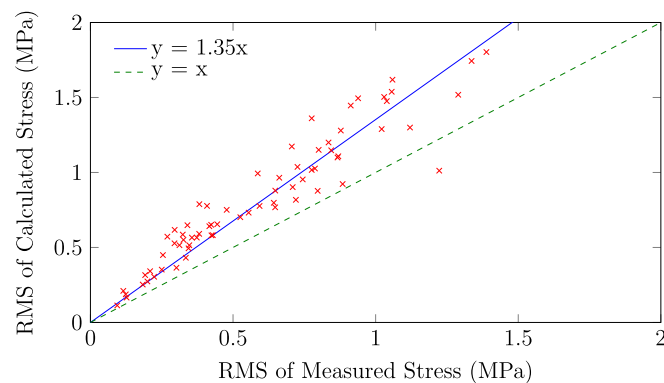
Comparison of calculated and measured zero-upcrossing frequency (STRUC_R result/gauge measurement) for 1-d and 2-d wave spectra.

Strain Gauge	Regression slope		R^2		CV (RMSD)	
	1-d	2-d	1-d	2-d	1-d	2-d
15	0.77	0.90	0.90	0.99	0.38	0.15
17	0.88	0.89	0.91	0.98	0.32	0.17
18	0.85	1.02	0.92	0.99	0.31	0.12
19	0.73	0.94	0.90	0.99	0.39	0.11
20	0.76	0.92	0.90	0.99	0.38	0.13
26	0.83	0.94	0.91	1.00	0.33	0.10
27	0.84	1.00	0.90	0.99	0.33	0.09
28	0.85	1.01	0.91	0.99	0.32	0.08
29	0.84	0.96	0.90	1.00	0.33	0.08
30	0.86	0.95	0.92	0.99	0.31	0.09
33	0.84	0.98	0.91	0.99	0.33	0.09
34	0.82	1.01	0.90	0.99	0.34	0.10
35	0.82	1.01	0.91	0.99	0.33	0.09
37	0.85	0.97	0.91	0.99	0.33	0.09
Avg	0.82	0.96	0.91	0.99	0.34	0.11
Std dev	0.04	0.04	0.01	0.00	0.03	0.03
Min	0.73	0.89	0.90	0.98	0.31	0.08
Max	0.88	1.02	0.92	1.00	0.39	0.17

Table 4

Comparison of damage estimates (STRUC_R result/result based on gauge measurements) for 1-d and 2-d wave spectra.

Strain Gauge	Regression slope		R^2		CV (RMSD)/Gauge		Ratio of sum of damage estimates	
	1-d	2-d	1-d	2-d	1-d	2-d	1-d	2-d
15	4.67	2.16	0.90	0.93	7.68	2.51	3.98	2.41
17	0.99	0.45	0.76	0.77	0.72	0.78	0.97	0.56
18	0.51	0.36	0.43	0.80	1.11	0.96	0.54	0.48
19	0.27	0.20	0.89	0.89	1.70	1.86	0.28	0.27
20	0.47	0.21	0.86	0.86	1.24	1.74	0.47	0.31
26	1.84	0.90	0.87	0.97	2.12	0.36	1.51	0.92
27	1.72	1.13	0.31	0.86	3.55	0.63	1.68	1.26
28	1.60	1.11	0.31	0.87	3.26	0.58	1.61	1.22
29	1.49	0.73	0.87	0.96	1.43	0.59	1.23	0.75
30	1.82	0.91	0.86	0.97	2.02	0.34	1.51	0.93
33	3.04	1.48	0.84	0.97	4.39	1.02	2.44	1.48
34	0.90	0.62	0.30	0.88	1.87	0.60	0.92	0.69
35	0.98	0.65	0.38	0.88	1.70	0.57	0.94	0.71
37	3.09	1.49	0.86	0.97	4.52	1.04	2.52	1.52
Avg	1.67	0.89	0.67	0.90	2.67	0.97	1.47	0.97
Std dev	1.22	0.55	0.26	0.06	1.87	0.64	0.98	0.58
Min	0.27	0.20	0.30	0.77	0.72	0.34	0.28	0.27
Max	4.67	2.16	0.90	0.97	7.68	2.51	3.98	2.41

**Fig. 5.** RMS longitudinal stress results for gauge s15 using 2-d wave spectra. The best-fit line and line of exact agreement are shown.

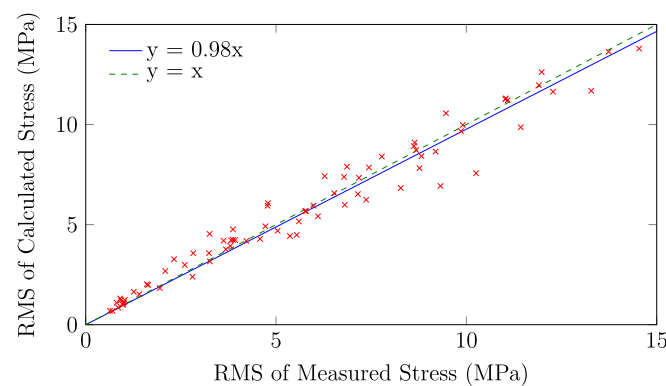


Fig. 6. RMS longitudinal stress results for gauge s26 using 2-d wave spectra. The best-fit line and line of exact agreement are shown.

4.3. Comparison between gauges for all wave spectrum models

The agreement between measurements and calculations for each gauge tended to be quite consistent between spectrum models, particularly with respect to the outliers. The poorest RMS stress results were consistently with gauge s15 (example shown in Fig. 5), which also had the lowest RMS stress values amongst the 14 gauges. Each of the gauges near the bow (s15–s20) tended to have poorer agreement with measurements. These gauges experienced stresses that were less than half those of the remaining strain gauges. If the results of gauges s15–s20 are removed from the RMS stress and zero-upcrossing frequency analysis, the average of each statistic moves closer to unity except the CV(RMSD) values which are reduced in value. Each of these changes indicates better agreement with measurements. It is believed the poorer performance of gauges near the bow was due in part to absolute errors in measurements and calculations causing more relative error at low strain measurements.

4.4. Comparison of results using 1-d and 2-d wave spectra

The results shown in Table 2 show reasonable agreement between calculated and measured values of RMS longitudinal stress when using 1-d and 2-d wave spectra. The regression slope shows, on average, slight underprediction of RMS stress but both the 1-d and 2-d results contain trial runs with slopes 30% greater than or less than unity. The average result is slightly better using the 1-d wave spectrum model but the magnitude of the outliers is lower for the 2-d results. The regression slopes from both 1-d and 2-d results are consistent with the analysis of the United States Coast Guard maritime cutters which found the calculated vertical bending moments were typically within 25% of the measured values [13], however, no significant amount of bias was observed in this study. The coefficient of determination shows both the 1-d and 2-d results fit the best-fit lines well but less scatter is present in the 2-d results. The difference between calculated and measured results, as assessed using CV(RMSD) (Eq. (4)), shows that the 2-d results are in better agreement with measurements for all gauges except s30, which has similar results using the 1-d and 2-d spectra. Overall, the 2-d RMS stress results have CV(RMSD) values approximately 45% lower than the 1-d results.

The 1-d and 2-d zero-upcrossing frequency values show good agreement with measured values in Table 3. The regression slopes show less variation between gauges than is seen for the RMS stress. The 1-d regression slopes are consistently about 20% lower than measurements and the 2-d results show the same consistency between gauges but are only about 5% lower than measurements. Very little scatter was observed in the 2-d results (as seen in Figs. 7 and 8), consistent with the high R^2 values. The 1-d R^2 values were about 10% lower, indicating more, but still limited scatter and good agreement with the best-fit line. The CV(RMSD) values for the 2-d were one-third those of the 1-d results, indicating that although the 1-d results agreed well with measurements, the 2-d results agreed substantially better.

The damage estimates were calculated using Eq. (3). It shows that while other terms are held constant, damage is proportional to the zero-upcrossing frequency multiplied by the m -th power of the square root of the zeroth spectral moment where m is the negative inverse of the slope of the S-N curve. Since the RMS stress is estimated as $\sqrt{M_0}$ and m is set to three, this means the RMS stress values are cubed, emphasizing discrepancies between measured and calculated values of RMS stress. This is consistent with the damage estimate comparisons for 1-d and 2-d spectra shown in Table 4 which shows much poorer agreement with estimates based on measurements than were seen with either RMS stress or zero-upcrossing frequency.

The slope of the best-fit lines for the 1-d damage estimate results was 1.67 on average, but there were significant outliers. The regression slopes for the 2-d results were better as the average showed an underprediction of about 10%, but the outliers were still significant. The minimum and maximum were 0.20 and 2.16, respectively. The R^2 values for the damage estimate comparisons were lower than those for the RMS stress and zero-upcrossing frequency for each of the spectrum models. The 2-d results showed less scatter within the results for each gauge and between gauges. Since the 2-d results showed less scatter

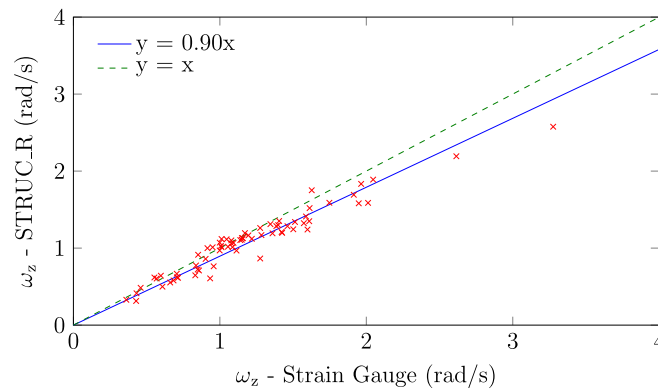


Fig. 7. Zero-upcrossing frequency results for gauge s15 using 2-d wave spectra. The best-fit line and line of exact agreement are shown.

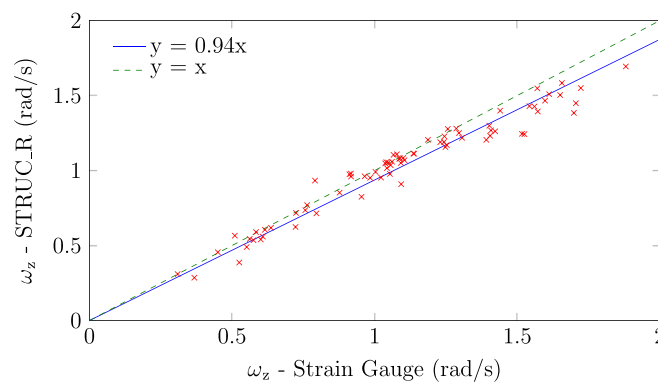


Fig. 8. Zero-upcrossing frequency results for gauge s26 using 2-d wave spectra. The best-fit line and line of exact agreement are shown.

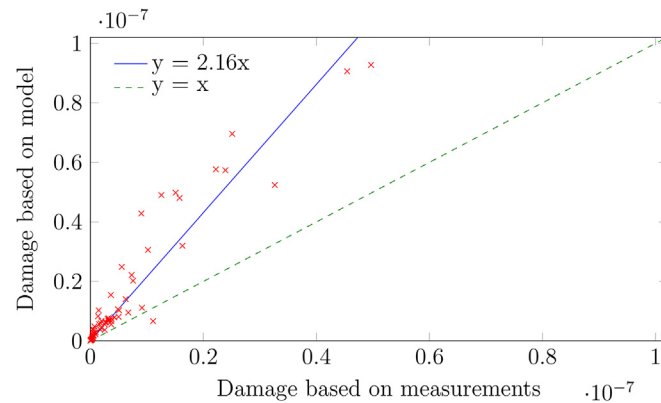


Fig. 9. Damage estimate results for gauge s15 using 2-d wave spectra. The best-fit line and line of exact agreement are shown.

and regression slopes closer to unity, it is not surprising that the CV(RMSD) values are substantially lower than those for the 1-d results. The average and standard deviation of CV(RMSD) values for the 2-d results were approximately one-third those of the 1-d results. Since the RMS stress results are cubed, it was expected that these values would also be greater than the respective RMS stress and zero-upcrossing frequency values.

The sum of the damage estimates based on calculations over all the trial runs was divided by the sum of damage estimates based on measurements. This statistic is meaningful for a fatigue assessment, as it emphasizes the impact of conditions that would cause fatigue damage. These results are somewhat better than those of the regression slopes, showing a 47%

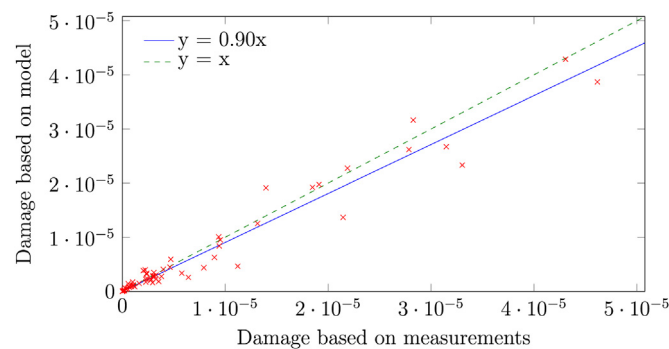


Fig. 10. Damage estimate results for gauge s26 using 2-d wave spectra. The best-fit line and line of exact agreement are shown.

overprediction and 3% underprediction on average for the 1-d and 2-d results, respectively, with several outliers for each wave spectrum model.

4.5. Comparison of results with spreading functions

The results from the wave spectrum models using a 90° spreading angle and the measured spreading angles are shown in Tables 5 and 6, respectively. The two spectrum models yielded very similar results. The differences between the RMS stress and zero-upcrossing frequency statistics for individual gauges typically varied by less than 5% between the two spectrum models with only slightly more variation between gauges in the damage estimate calculations. Although the results of the spreading functions gave very similar results, there was a reasonable difference between the spreading angles considered. One spreading function used a constant 90° spreading angle while the other had an average of 98° and almost half the trial runs had spreading angles more than 25° greater than or less than 90° .

The spectrum models using a spreading function generated RMS stress results that were consistent with the 1-d and 2-d results. The best-fit line slopes were similar while the R^2 values were closer to those of the 2-d results than the 1-d results. The average CV(RMSD) was 0.32 for the 1-d with 90° spreading angle compared to 0.46 for the 1-d results and 0.25 for the 2-d results.

The zero-upcrossing frequency results of the models with spreading functions were quite close to those of the 1-d results. There was a minor reduction in the CV(RMSD) values indicating better agreement with measured values but otherwise the statistics did not change much from the 1-d results.

Statistics related to damage estimates among the models with spreading functions fell between the 1-d and 2-d results with few exceptions. The use of a spreading function improved the average ratio of total fatigue damage estimate by approximately 10% (1.47 for 1-d, 1.29 for measured spreading angles, 1.32 for 90° spreading angles). The regression slopes and CV(RMSD) values suggest the models with spreading functions gave results with agreements between the 1-d and 2-d models. The statistics of the models with spreading functions were typically improved from the 1-d results by about one-third of the difference between 1-d and 2-d statistics.

5. Conclusions

The methodology of combining linear frequency-domain hydrodynamic loads with a linear finite element (FE) solver generated stress spectra parameters and damage estimates that were in good agreement with values derived from measurements for each of the four wave spectrum models. The instrumented areas are not prone to fatigue damage, so the stresses were relatively low which can result in greater relative error in the measurement of strains. In that way, this study is conservative with respect to the agreement that could be expected between the same calculated and measured parameters of areas more likely to experience fatigue damage. The agreement between measured and calculated values indicates that reasonable stress spectra and corresponding fatigue damage estimates can be calculated using this method for a naval vessel.

The results from the 2-d wave spectra clearly agree with measurements better than the other wave spectrum models. This was expected as it is a better representation of the seaway than the other methods. The 1-d results had the poorest agreement with measurements and the two models using a spreading function gave very similar results, both better than 1-d results but not as good as the 2-d results. The use of more accurate seaway representations improved the agreement of each calculated parameter with those of measurements but similar conclusions could be drawn with each of the spectrum models. This is encouraging because typically, spectral fatigue analyses are performed using wave statistics which only report significant wave height and period. The similarity between the results using a measured spreading angle and 90° as the spreading angle suggests the extra effort to determine the distribution of spreading angles does not give corresponding better results and suggests the use of 90° as the spreading angle is justified. Therefore, the addition of a spreading function to a wave spectrum model where only significant wave height and period are available may yield better results without a great deal of additional

Table 5

Comparison of calculated and measured parameters (STRUC_R result/gauge measurement) for 1-d with 90° spreading angle wave spectra.

Parameter	Statistic	Regression slope	R^2	CV (RMSD)	Total damage ratio
RMS stress	Avg	0.98	0.96	0.31	—
	Std dev	0.20	0.01	0.10	—
	Min	0.65	0.94	0.20	—
	Max	1.41	0.97	0.57	—
ω_z	Avg	0.83	0.94	0.29	—
	Std dev	0.06	0.01	0.05	—
	Min	0.72	0.92	0.23	—
	Max	0.92	0.96	0.36	—
Damage	Avg	1.41	0.83	1.71	1.29
	Std dev	0.89	0.09	1.27	0.80
	Min	0.21	0.68	0.45	0.25
	Max	3.51	0.94	5.24	3.29

Table 6

Comparison of calculated and measured parameters (STRUC_R result/gauge measurement) for 1-d with measured spreading angle wave spectra.

Parameter	Statistic	Regression slope	R^2	CV (RMSD)	Total damage ratio
RMS stress	Avg	0.99	0.96	0.32	—
	Std dev	0.20	0.01	0.10	—
	Min	0.64	0.94	0.21	—
	Max	1.41	0.97	0.58	—
ω_z	Avg	0.84	0.95	0.27	—
	Std dev	0.05	0.01	0.05	—
	Min	0.74	0.93	0.21	—
	Max	0.91	0.97	0.35	—
Damage	Avg	1.46	0.81	1.87	1.31
	Std dev	0.95	0.10	1.40	0.82
	Min	0.21	0.65	0.48	0.25
	Max	3.72	0.91	5.76	3.38

computational expense or effort. In this study, the agreement with measurements (measured by reduction of CV(RMSD)) improved by 30% for RMS stress, 21% for zero-upcrossing frequency, and 36% for damage estimates by adding a spreading function to the 1-d spectra. Use of 2-d wave spectra is desirable, but this is only possible for an analysis conducted after the waves have been measured. The cost and complexity of measuring waves while monitoring fatigue damage on a ship will determine if this is feasible.

A 2-d wave spectrum will typically provide a better representation of the seaway than a 1-d spectrum based on two measured parameters. A better representation of the seaway can aid in providing more accurate calculations of the stress conditions. The differences between calculations of stress spectra and fatigue damage estimates using 1-d and 2-d wave spectra will be partly dependent on the degree of spreading and how well the 1-d wave spectrum model describes the seaway. It is difficult to draw general conclusions based on a sea trial that lasted several days as the ship would only experience a limited range of different sea conditions.

There are a number of parameters that introduce uncertainty into spectral fatigue analysis, including nonlinear behavior in hydrodynamics and structural response, operational profile, and seaway representation which includes the selection of a wave spectrum model. The results of this study suggest that better seaway representations improve a spectral fatigue analysis, but the use of 1-d wave spectra can generate reasonable estimates of RMS stress, zero-upcrossing frequency, and associated damage estimates. Future work is required to better understand the significance of other parameters in the fatigue life of naval vessels. Future work is also needed to compare spectral damage predictions with rainflow damage predictions from the measured data as well as comparisons between measured and calculated ship motions.

Acknowledgments

Thanks to many members of the Warship Performance section at DRDC Atlantic Research Centre for their assistance, especially James Nickerson, for his work improving the STRUC_R software.

References

- [1] Ashe G, Cheng F, Kaeding P, Kaneko H, Dow R, Broekhuijsen J, et al. ISSC committee v.5: naval ship design. In: 17th international ship and offshore structures congress, vol. 2. ISSC; 2009. p. 259–307.
- [2] Soares CG, Garbatov Y, von Selle H. Fatigue damage assessment of ship structures based on the long-term distribution of local stresses. Intern Shipbuild Prog 2003;50(1 & 2):35–55.
- [3] Lloyd's Register. ShipRight design and construction, fatigue design assessment: level 3 procedure. London, United Kingdom. 2009.

Please cite this article in press as: Thompson I, Validation of naval vessel spectral fatigue analysis using full-scale measurements, Marine Structures (2016), <http://dx.doi.org/10.1016/j.marstruc.2016.05.006>

- [4] Det Norske Veritas. Fatigue assessment of ship structures: classification notes No. 30.7. 2014.
- [5] Bureau Veritas. Spectral fatigue analysis methodology for ships and offshore units: guidance note NI 539 DT R00 E. 2008.
- [6] Fricke W, Cui W, Kierkegaard H, Kihl D, Koval M, Mikkola T, et al. Comparative fatigue strength assessment of a structural detail in a containership using various approaches of classification societies. *Mar Struct* 2002;15:1–13.
- [7] Kukkanen T, Mikkola TP. Fatigue assessment by spectral approach for the ISSC comparative study of the hatch cover bearing pad. *Mar Struct* 2004;17:75–90.
- [8] Park TY, Jang CD, Suh YS, Kim BJ. A parametric study based on spectral fatigue analysis for 170k LNGC. *Intern J Nav Archit Ocean Eng* 2011;3:116–21.
- [9] Wang Y. Spectral fatigue analysis of a ship structural detail - a practical case study. *Intern J Fatigue* 2010;32:310–7.
- [10] Drummen I, Storhaug G, Moan T. Experimental and numerical investigation of fatigue damage due to wave-induced vibrations in a containership in head seas. *J Mar Sci Technol* 2008;13(4):428–45.
- [11] Li Z, Mao W, Ringsberg JW, Johnson E, Storhaug G. A comparative study of fatigue assessments of containership structures using various direct calculation approaches. *Ocean Eng* 2014;82:65–74.
- [12] Drummen I, Schiere M, Dallinga R, Stambaugh K. Full scale trials, monitoring and model testing conducted to assess the structural fatigue life of a new US coast guard cutter. In: *Ship structure committee 2014 symposium*. Ship Structure Committee; 2014. p. 18–20.
- [13] Hageman R, Drummen I, Stambaugh K, Dupau T, Herel N, Derbanne Q, et al. Structural fatigue loading predictions and comparisons with test data for a new class of US coast guard cutters. In: *Ship structure committee 2014 symposium*. Ship Structure Committee; 2014. p. 1–11.
- [14] Garbatov Y, Soares CG. Uncertainty assessment of fatigue damage of welded ship structural joints. *Eng Struct* 2012;44:322–33.
- [15] Thompson I. Influence of sea state models on calculated naval vessel stress spectra. In: *Proceedings of the 18th international conference on ships and shipping Research*; 2015. p. 428–36.
- [16] van Daalen EFG, Sireta FX. PRECAL_R user manual. MARIN. 2014.
- [17] Thompson I, Stredulinsky D, Gannon L, Oakley S. STRUC_R v. 2.4 user's manual. External Client Report 2013-026. DRDC Atlantic; 2013.
- [18] Martec Limited. Vibration and strength analysis program (VAST) version 9.0 User's manual. 2006.
- [19] Stansberg CT, Contento G, Hong SW, Irani M, Ishida S, Mercier R, et al. The specialist committee on waves final report and recommendations to the 23rd ITTC. In: *Proceedings of the 23rd ITTC*, vol. II; 2002. p. 505–51.
- [20] Det Norske Veritas. Recommended practice DNV-RP-C102, structural design of offshore ships. 2002.
- [21] Eisenhauer JG. Regression through the origin. *Teach Stat* 2003;25(3):76–80.